

Supplementary Information for
A curtain purification system based on rabbit fur-based
rotating triboelectric nanogenerator for efficient
photocatalytic degradation of volatile organic compounds

Dehong Yang^{‡a}, Zhaoqi Liu^{‡bc}, Peng Yang^{bc}, Ling Huang^a, Fengjiao Huang^a, Xinglin Tao^{bc},
Yuxiang Shi^{bc}, Rui Lei^b, Jiazhen Cao^d, Hexing Li^{ae}, Xiangyu Chen^{*bc}, Zhenfeng Bian^{*a}

^a MOE Key Laboratory of Resource Chemistry and Shanghai Key Laboratory of Rare Earth Functional Materials, Shanghai Normal University, Shanghai 200234, China.

^b CAS Center for Excellence in Nanoscience, Beijing Key Laboratory of Micro-nano Energy and Sensor, Beijing Institute of Nanoenergy and Nanosystems, Chinese Academy of Sciences, Beijing 100083, China.

^c College of Nanoscience and Technology, University of Chinese Academy of Sciences, Beijing 100049, China.

^d Key Laboratory for Advanced Materials and Joint International Research Laboratory of Precision Chemistry and Molecular Engineering, School of Chemistry and Molecular Engineering, East China University of Science and Technology, Shanghai 200237, China.

^e Shanghai University of Electric Power, Shanghai 200090, China.

[‡] Dehong Yang and Zhaoqi Liu contributed equally to this work.

* To whom correspondence should be addressed: chenxiangyu@binn.cas.cn

bianzhenfeng@shnu.edu.cn

The PDF file includes:

Fig. S1 to S13

Other Supplementary Material for this manuscript includes the following:

Videos S1 and S2

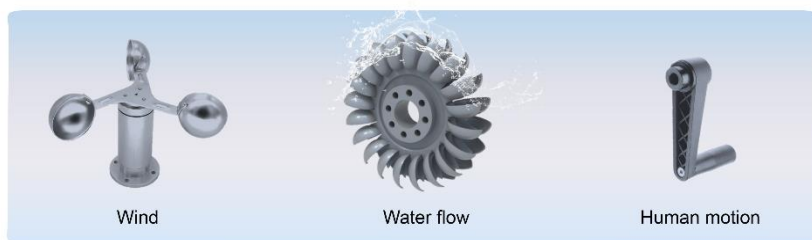


Fig. S1 Energy forms driving RR-TENG, which has wind, water flow and human motion.

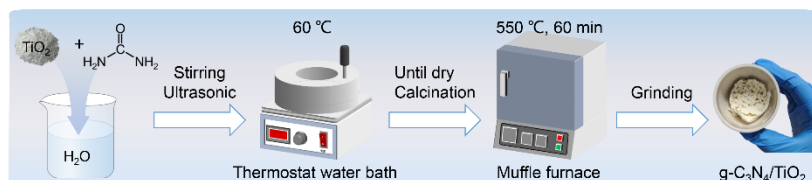


Fig. S2 Preparation illustration of g-C₃N₄/TiO₂ composite photocatalyst.

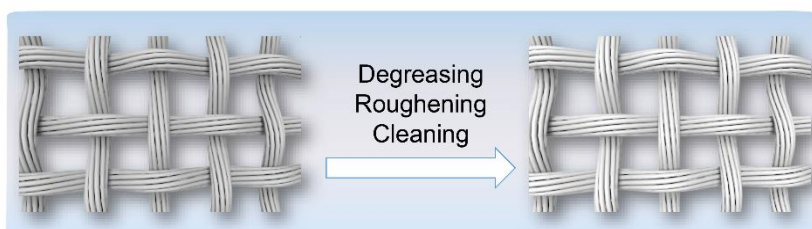


Fig. S3 Flowchart of commercial fabric pretreatment.

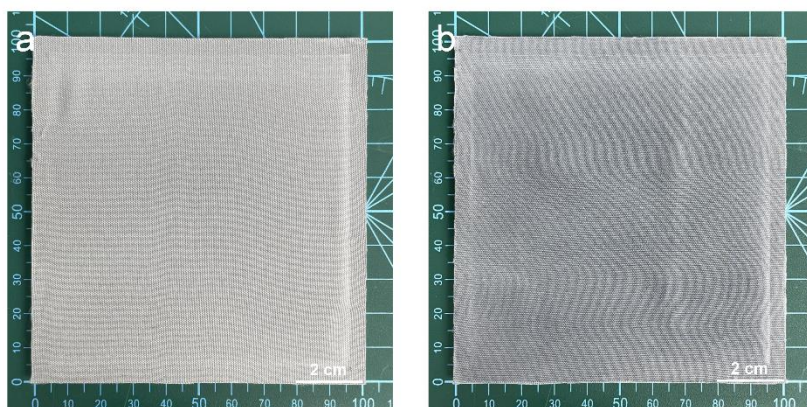


Fig. S4 Photographs of (a) pretreated commercial fabric, (b) conductive curtain with photocatalysis (finished product), scale bar, 2 cm.

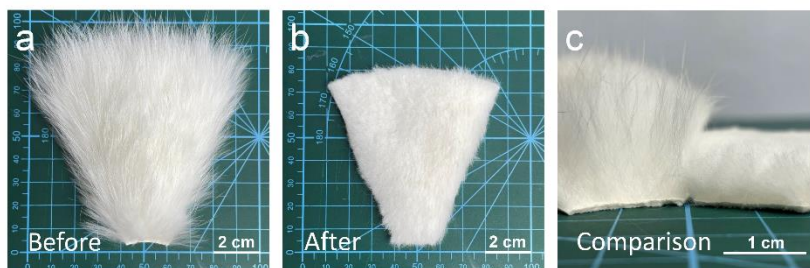


Fig. S5 Photographs of rabbit fur before and after trimming and its effect comparison. (a)

Untreated rabbit fur (before trimming), (b) treated rabbit fur (after trimming), scale bar, 2 cm. (c)
Effect comparison of rabbit fur, scale bar, 1 cm.

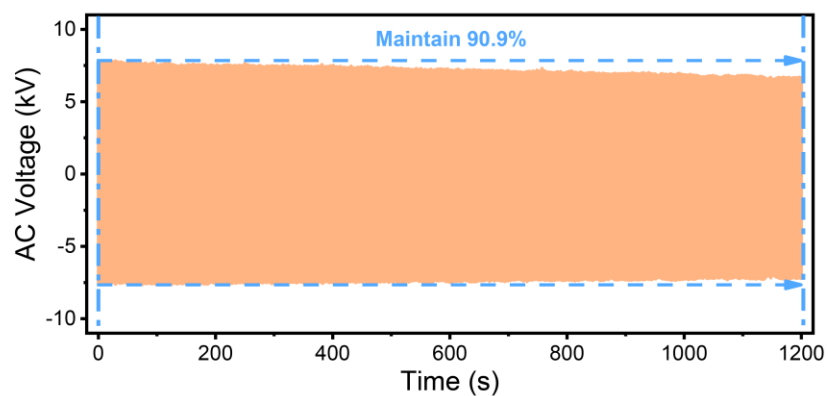


Fig. S6 Voltage stability test of RR-TENG running for 2000 times.

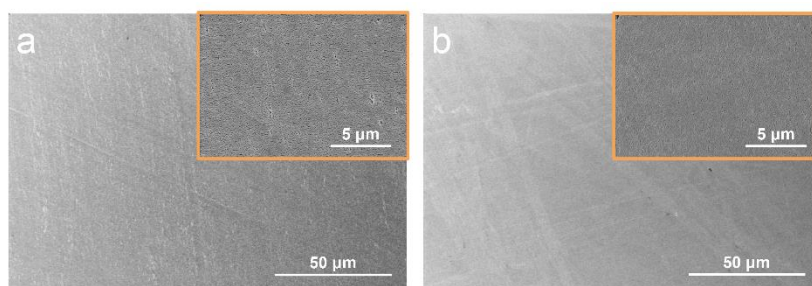


Fig. S7 Microscopic surface morphology of PTFE before (a) and after (b) friction, scale bar, 50 μm (inset, scale bar, 5 μm).

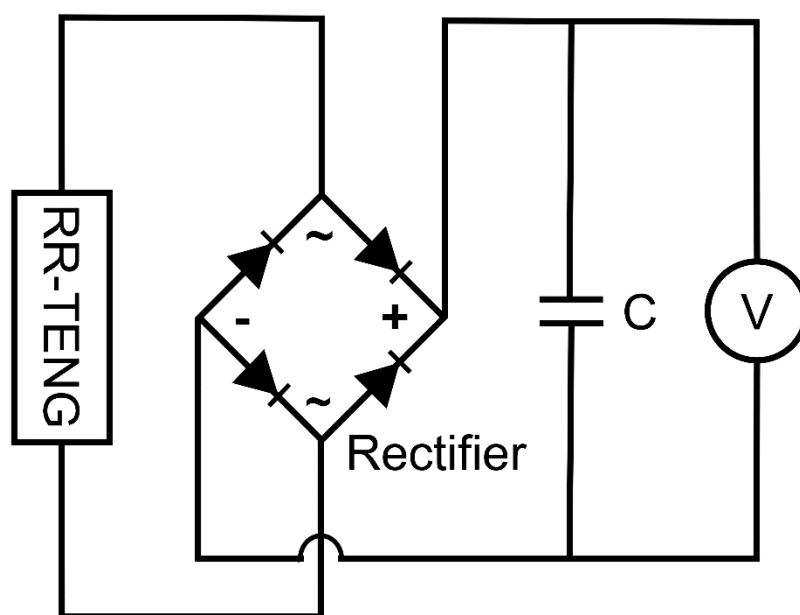


Fig. S8 Circuit diagram of charging commercial capacitor.



Fig. S9 Photograph of simulated reaction chamber for formaldehyde reaction (quartz glass on the right, 9 L), scale bar, 10 cm.

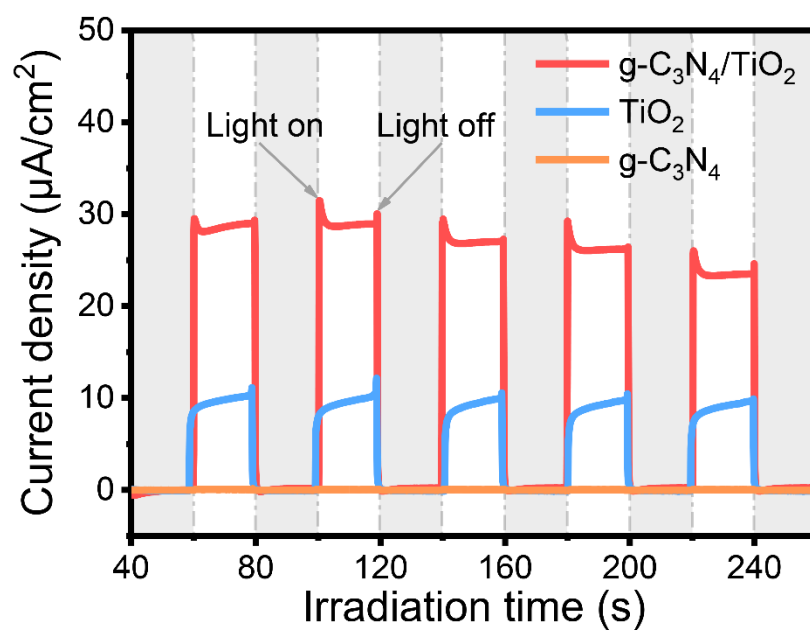


Fig. S10 Photocurrent response spectrum of photocatalysts ($\lambda=365$ nm).

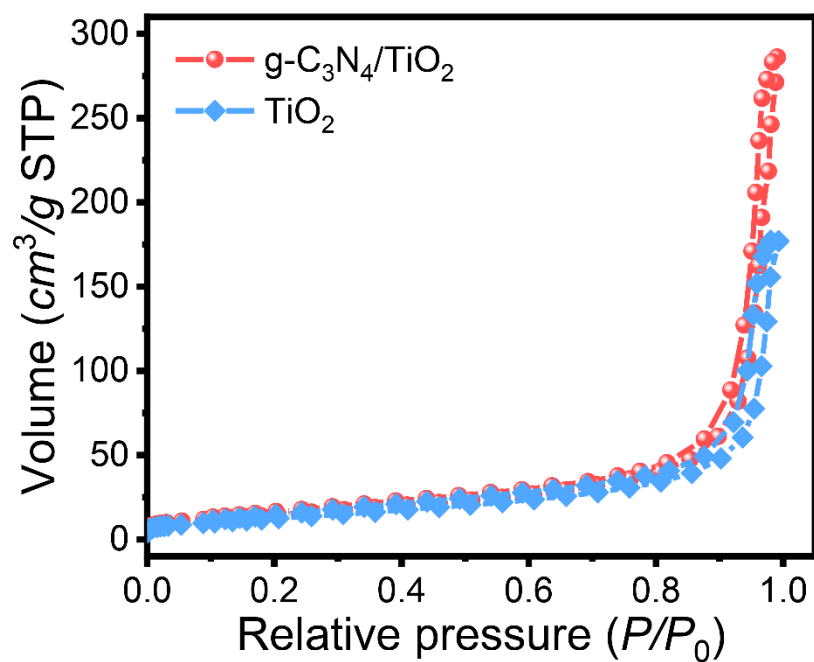


Fig. S11 BET surface area spectra of g-C₃N₄/TiO₂ and TiO₂ photocatalyst.

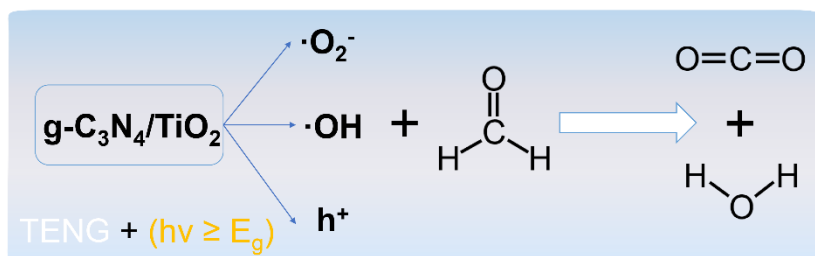


Fig. S12 Reaction path of formaldehyde degradation.

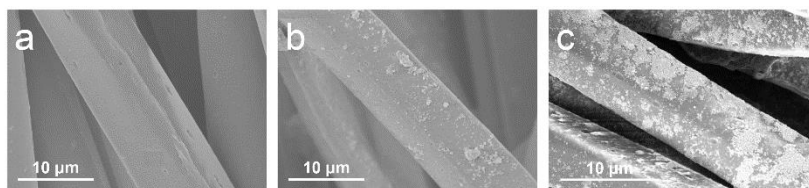


Fig. S13 SEM images before and after dust removal. SEM images of (a) conductive curtain, (b) conductive curtain with photocatalyst (before removing smoke), (c) conductive curtain containing photocatalyst and PM (after removing smoke), scale bar, 10 μm .